Available online at www.sciencedirect.com

ScienceDirect

Procedia Computer Science 60 (2015) 1289 – 1298

Procedia Computer Science

19th International Conference on Knowledge Based and Intelligent Information and Engineering Systems

The role of path continuity in lateral vehicle control

Mohamed Elbanhawi*, Milan Simic, Reza Jazar

School of Aerospace, Mechanical and Manufacturing Engineering, RMIT University
Bundoora East Campus, PO Box 70, Bundoora, Victoria, 3083, Australia

Abstract

Motion planning and tracking control are generally developed separately for autonomous vehicle's navigation. Paths are often designed to satisfy the kinematics of the vehicle. Geometric singularities in the reference trajectory deteriorate the performance of the path tracking controller. An integrated approach is needed in autonomous robotics research to account for the influence of the path properties on the controller behavior. The current research considers the controller performance and resulting stability and disturbances of the vehicle. The compound effect of planning and tracking control is investigated in this article. Systematic changes to the vehicle velocity, desired maneuver and tracking algorithm are made to evaluate the role of path planning continuity on the vehicle's dynamic responses and controller's performance. This research validates previous literature that showed enhancement in controller performance by using continuous reference trajectories. Our findings suggest that the use of cubic parametrically continuous spline paths improves passenger comfort and enhance vehicle's stability. The experimental results report a 90% reduction in both lateral acceleration and side slip.

Peer-review under responsibility of KES International

Keywords: path planning; path tracking; lateral control; autonomous vehicles, self-driving; tracking control

* Corresponding author. Tel.: +61 03 9925 6242
E-mail address: mohamed.elbenhawi@rmit.edu.au

Peer-review under responsibility of KES International
doi:10.1016/j.procs.2015.08.194

1. Introduction

Autonomous passenger vehicles are expected to reduce the risk of driving and improve traffic flow efficiency. The majority of traffic accidents are related to human error and unintended lane departure[1]. Advanced Driver Assistance Systems (ADAS) such as forward warning collision, adaptive cruise control and lane departure warning were introduced to reduce driver task load and minimize consequent errors to mitigate accident risks. Autonomous passenger vehicle wide scale deployment is expected to be an evolution of ADAS research. The operation of autonomous agents is generally divided into Sense Plan Act (SPA) stages. This article is concerned with analyzing the compound role of path planning (plan) and tracking control (act) on the vehicle stability and resulting disturbances acting on a passenger vehicle.

Nomenclature

a	acceleration
a_i	distance from axel to centre of gravity
C	force coefficient
D	moment coefficient
e	error
$E_{x,y}$	controller error
E_ϕ	controller effort
F	force
I	moment of inertia
k	curvature
L	wheelbase
m	mass
r	radius of curvature
t	time
v	velocity
x, y	vehicle position
β	side slip angle
θ	heading angle
ω	yaw rate
ϕ	steering angle

2. Vehicle Model

2.1. Kinematics

In this study, the vehicle lateral motion and control are investigated. Therefore roll and pitch motions are ignored by assuming flat terrain and ignoring suspension effects. Independent longitudinal control is also assumed, since in on structured streets predominantly constant velocity is maintained. Bicycle model is widely accepted for representing a front wheel steering vehicle's global planar motion[2, 3]. The vehicle's kinematic configuration is described by its pose, i.e. position, (x, y) and heading, θ. The pose is measured between the global frame and a body frame in the center of rear axle. Front wheels control the steering and the rear wheels are fixed. A single steering angle, ϕ, can be used to represent the vehicle's steering by averaging left and right steering wheels' angles. Velocity, v, and steering angle, ϕ, are the two control commands for the considered model. The Model is given by equation (1). Steering is restricted to a maximum angle value of ϕ_{max}, which in turn limits the curvature, k, of the motion path as expressed in equation (2), where L is the distance between the front and rear axles, r is the radius of curvature and Δt is the time step.

$$\begin{cases} x_{i+1} = x_i + v_i . cos(\theta_i) . \Delta t \\ y_{i+1} = y_i + v_i . sin(\theta_i) . \Delta t \\ \theta_{i+1} = \theta_i + v_i . \frac{tan(\phi_i)}{L} . \Delta t \end{cases} \quad (1)$$

$$k_{max} = \frac{1}{r_{min}} = \frac{tan(\phi_{max})}{L} \quad (2)$$

2.2. Lateral dynamics

The vehicle can be dynamically modeled as a rigid three degree of freedom system operating in a two dimensional environment. Three relevant motions in this article are longitudinal, lateral and yaw, which are expressed by v_x, v_y and ω. The corresponding dynamic equations of motions are formulated in (3), (4) and (5)[4], where m is the vehicle mass, a is the axle distance from the center of gravity, C is the wheel coefficient and F is the longitudinal force.

$$\dot{v}_x = \frac{F_x}{m} + \omega v_y \quad (3)$$

$$\dot{v}_y = \frac{1}{m v_x} (-a_1 C_{\alpha f} + a_2 C_{\alpha r})\omega - \frac{1}{m v_x} (C_{\alpha f} + C_{\alpha r}) v_y + \frac{1}{m} C_{\alpha f} \phi - \omega v_x \quad (4)$$

$$\dot{\omega} = \frac{1}{I_z v_x} (-a_1^2 C_{\alpha f} - a_2^2 C_{\alpha r})\omega - \frac{1}{I_z v_x} (a_1 C_{\alpha f} - a_2 C_{\alpha r}) v_y + \frac{1}{I_z} a_1 C_{\alpha f} \phi \quad (5)$$

2.3. Steady state responses

Steady state conditions are assumed as the vehicle is turning. For path planning and execution purposes, steady state responses were found to be sufficiently accurate to model the vehicle's motion when compared to transient dynamic equations[5]. Transient equations of motion are rather exhaustive to analytically compute for different paths with no notable difference. The steady state output responses of the vehicle to steering are derived as a functions of the vehicle parameters in equations (6)-(9)[4], where β is the side slip angle, C is the force coefficient and D is the moment coefficient.

$$\frac{\beta}{\phi} = \frac{D_\phi (C_\omega - m v_x) - D_\omega C_\phi}{D_\omega C_\beta - C_\omega D_\beta + m v_x D_\beta} \quad (6)$$

$$\frac{\omega}{\phi} = \frac{C_\phi D_\beta - C_\beta D_\phi}{D_\omega C_\beta - C_\omega D_\beta + m v_x D_\beta} \quad (7)$$

$$\frac{a}{\phi} = \frac{(C_\phi D_\beta - C_\beta D_\phi) v_x}{D_\omega C_\beta - C_\omega D_\beta + m v_x D_\beta} \quad (8)$$

$$\frac{v_y}{\phi} = \frac{D_\phi (C_\omega - m v_x) - D_\omega C_\phi}{D_\omega C_\beta - C_\omega D_\beta + m v_x D_\beta} v_x \quad (9)$$

3. Methodology

3.1. Experiments

Two experiments were used to evaluate the controllers' performance; both are commonly executed during on-road driving maneuvers. Case (1) is a right hand turn as shown in Fig. 1(a). It represents a step input or sudden change in the steering condition. Case (2) is the double lane change maneuver, illustrated Fig. 1(b). The double lane change standard test is used for assessing the stability of passenger vehicles[6]. In both cases, illustrated in Fig. 1, the start point is the bottom left end and example paths are colored in blue.

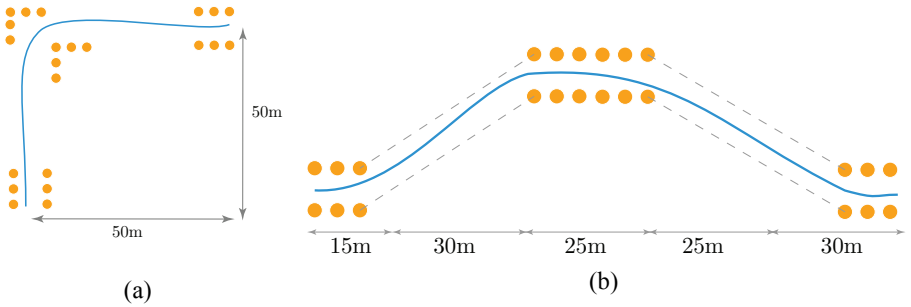

Fig. 1. (a) Testing manoeuvres right hand turn; (b) double lane change

3.2. Vehicle Parameters

The parameters of the vehicle used in the experiments are given in Table 1.

Table 1. Vehicle parameter values

Parameter	m [Kg]	I_z [Kg/m^2]	L [m]	a_1 [m]	a_2 [m]	C_{ar} [N/rad]	C_{af} [N/rad]	ϕ_{max} [deg]
Value	1000	1650	2.6	1.0	1.6	3000	3000	25

3.3. Path planning

Parametrically continuous paths are generated using clamped cubic non-uniform B-splines[7], as shown in Fig. 2. This algorithm generates paths with continuous steering, velocity and acceleration trajectories. Discontinuous paths are generated using Dubins paths that are combination of circular arcs and straight lines[8], as shown in Fig. 3. Both methods generate kinematically feasible paths with continuity.

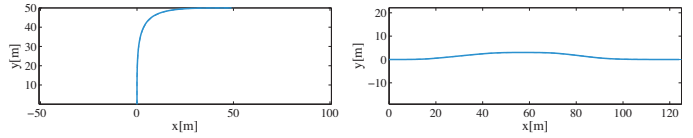

Fig. 2. (a) Continuous B-spline paths for left turn; (b) double lane change manoeuvres

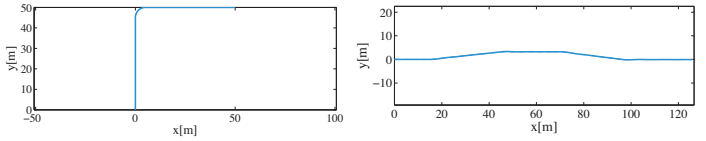

Fig. 3 (a) Discrete Dubins paths for left turn; (b) double lane change manoeuvres

3.4. Tracking control

The desired reference path is parameterized into a piecewise liner path connecting an infinitesimally close set of consecutive points. Pure pursuit algorithm was implemented, as it is the most common path tracking algorithm for mobile robots[9, 10]. It attempts to steer the vehicle towards a point on the path that is within a pre-determined look ahead distance, based on the tracking error. The desired heading at any instance j is calculated by equation (10) and the error, e, between current heading and desired heading, at the next step, is calculated by equation (11). Pure pursuit employs proportional control to compute the desired steering. For proportional control, the control gains in equation (12) are $K_p > 0$, $K_i = 0$ and $K_d = 0$. To improve the tracking performance, a PID controller was implemented by setting $K_p = 1.5$, $K_i = 1.0$ and $K_d = 0.2$.

$$\theta_j = atan\,\frac{y_i - y_{i-1}}{x_i - x_{i-1}} \tag{10}$$

$$e_j = \theta_{j+1} - \theta'_j \tag{11}$$

$$\phi_j = K_p e_j + K_i \int e\,dt + K_d \frac{de}{dt} \tag{12}$$

4. Results

The results are presented from a total of 24 numerical experiments. They were conducted for two cases (section 3.1), using two different controllers (section 3.4), and two path planners (section 3.3) at the three of longitudinal speeds (v = 1, 2.5 and 5 *m/s*). The mean tracking error (section 4.1) and controller effort (section 4.2) are used to evaluate path tracking controller's performance[9]. The steady state responses (section 4.3) are used to measure the stability of the vehicle and resulting disturbances.

4.1. Mean tracking error

The mean tracking error, $E_{x,y}$, between desired (x, y) and actual position (x', y') is calculated using equation (13), where N is the total number of points in the path. The errors for proportional pure pursuit are illustrated in Fig. 4 for the cases (1) and (2). PID pure pursuit results for case (1) and case (2) are given in Fig. 4 (c) and (d) respectively. Continuous B-spline path results are shown in red and Dubins steering results are blue.

$$E_{x,y} = \frac{1}{N}\sum_{i=0}^{N}\sqrt{(x_i - x'_i)^2 + (y_i - y'_i)^2} \tag{13}$$

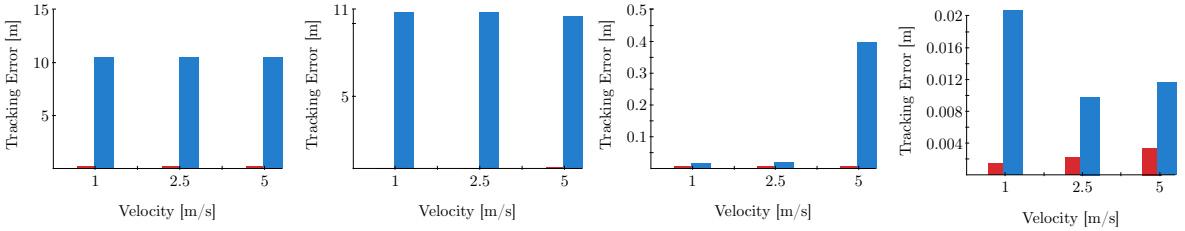

(a) Case (1) Proportional Controller (b) Case (1) PID Controller (c) Case (2) Proportional Controller (d) Case (2) PID Controller

Fig. 4. Mean tracking error for continuous (red) and discontinuous (blue) reference paths

4.2. Controller effort

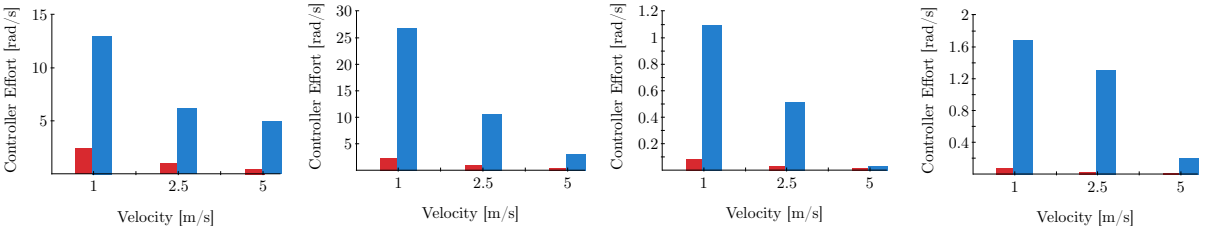

(a) Case (1) Proportional Controller (b) Case (1) PID Controller (c) Case (2) Proportional Controller (d) Case (2) PID Controller

Fig. 5. Controller effort for continuous (red) and discontinuous (blue) reference paths

The controller effort, E_ϕ, between desired (x, y) and actual position (x', y') is calculated using equation (14), where N is the total number of points in the path. The errors for proportional pure pursuit are illustrated in Fig. 5 for (a) case (1) and (b) case (2). PID pure pursuit results for case (1) and case (2) are given in Fig. 5 (c) and (d) respectively. Continuous B-spline path results are shown in red and Dubins steering results are blue.

$$E_\phi = \sum_{i=0}^{N} \frac{1}{2} \sqrt{\phi_i^2} \tag{14}$$

4.3. Dynamic responses

The responses of the vehicle to steering are calculated from equations (6)-(9). The results for proportional control for case (1) and case (2) are given in Fig. 6 and Fig. 8. The results for PID pursuit for case (1) and case (2) are given in Fig. 7 and Fig. 9. In all figures, (a), (c), (e) are continuous B-spline results and (b), (d), (f) are Dubins results.

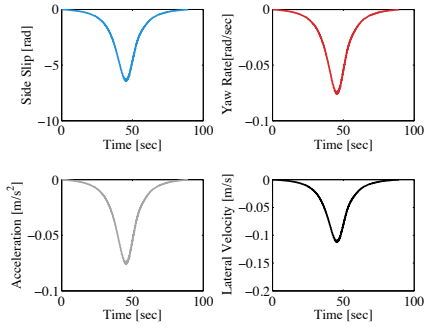

(a) v = 1 m/s

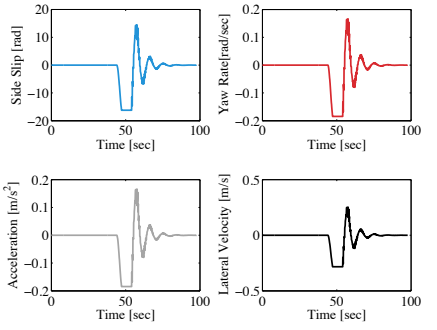

(b) v = 1 m/s

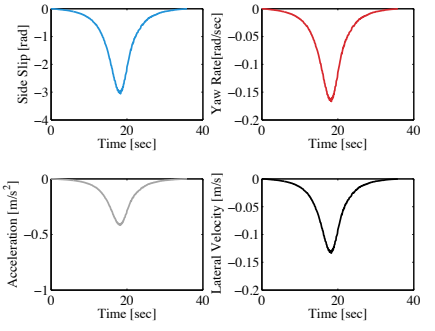

(c) v = 2.5 m/s

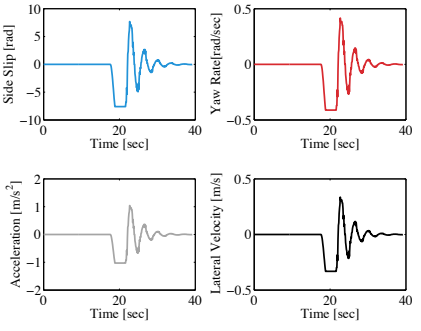

(d) v = 2.5 m/s

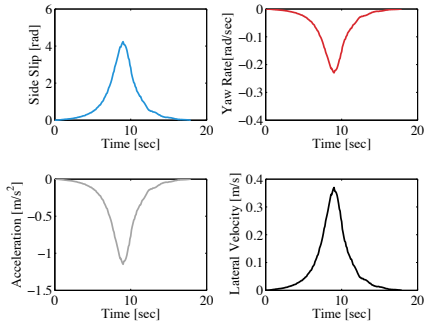

(e) v = 5 m/s

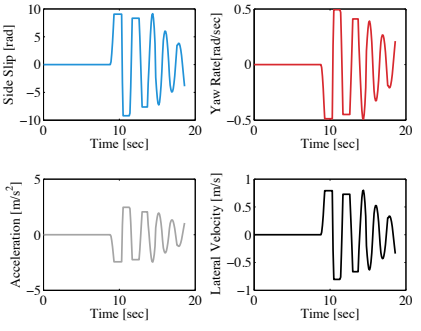

(e) v = 5 m/s

Fig. 6. Case (1) vehicle response to proportional tracking control of continuous (a)(c)(e) and discontinuous (b)(d)(f) paths

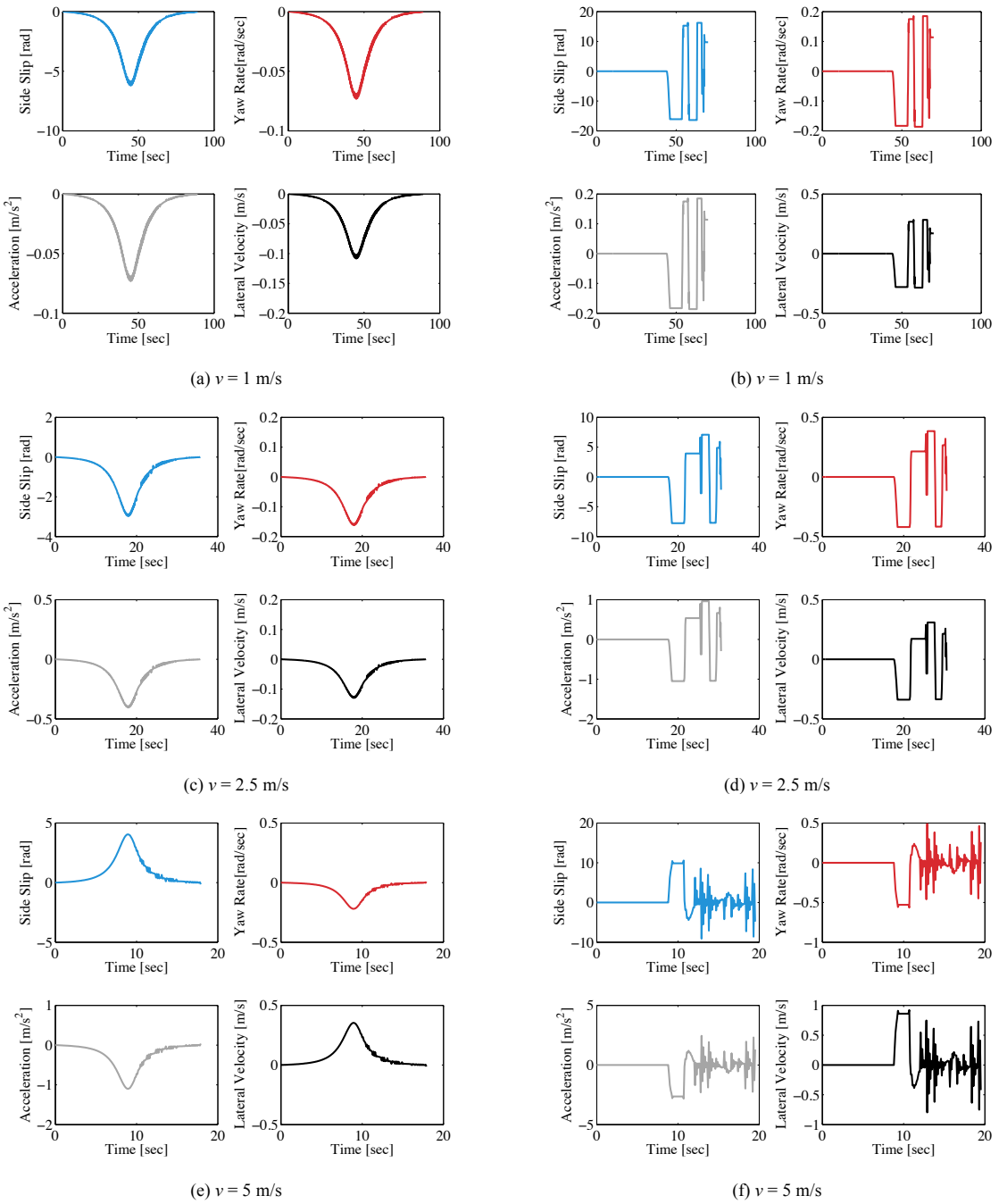

(a) v = 1 m/s (b) v = 1 m/s

(c) v = 2.5 m/s (d) v = 2.5 m/s

(e) v = 5 m/s (f) v = 5 m/s

Fig. 7. Case (1) vehicle response to PID tracking control of continuous (a)(c)(e) and discontinuous (b)(d)(f) paths

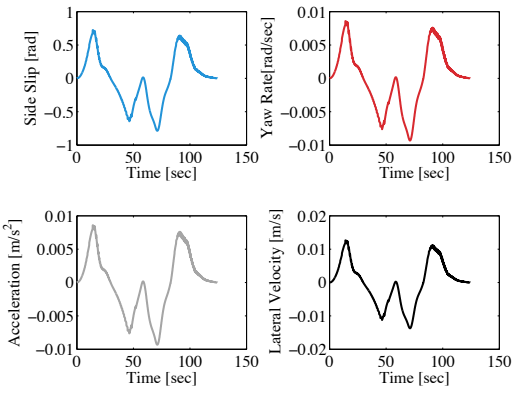

(a) v = 1 m/s

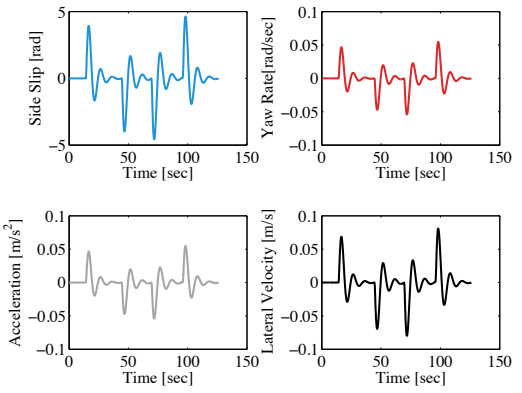

(b) v = 1 m/s

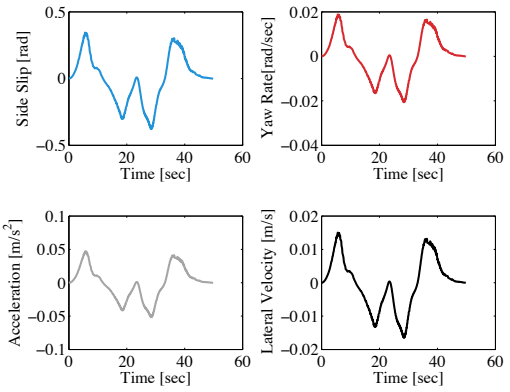

(c) v = 2.5 m/s

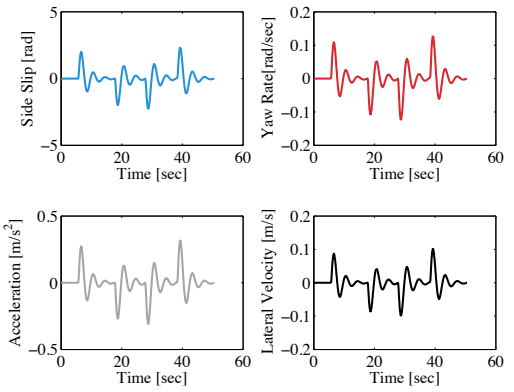

(d) v = 2.5 m/s

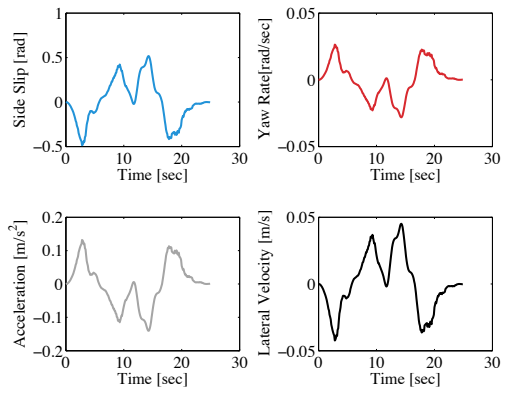

(e) v = 5 m/s

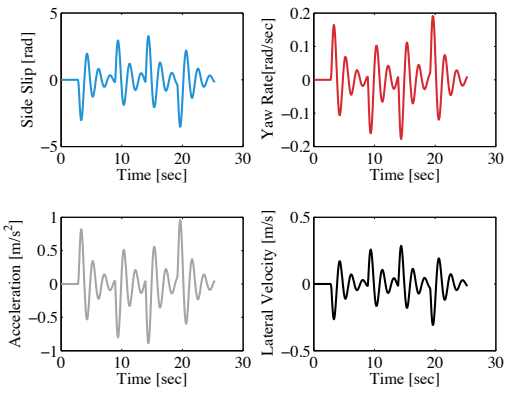

(f) v = 5 m/s

Fig. 8. Case (2) vehicle response to proportional tracking control of continuous (a)(c)(e) and discontinuous (b)(d)(f) paths

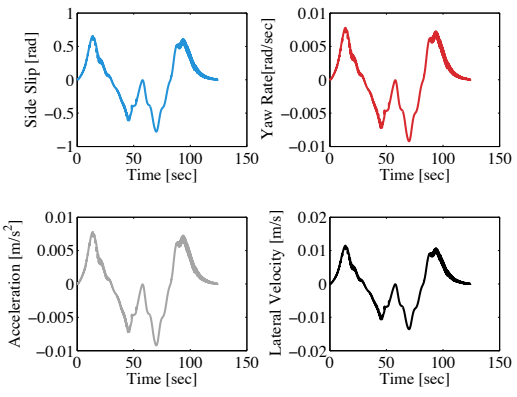

(a) v = 1 m/s

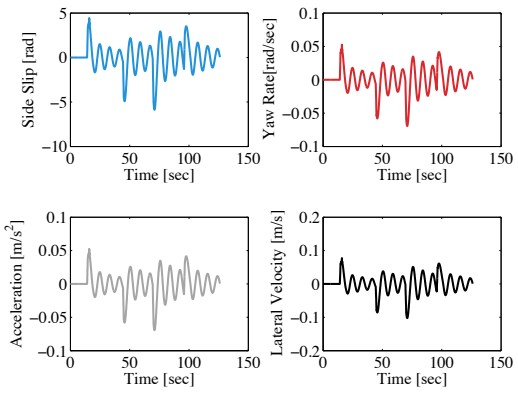

(b) v = 1 m/s

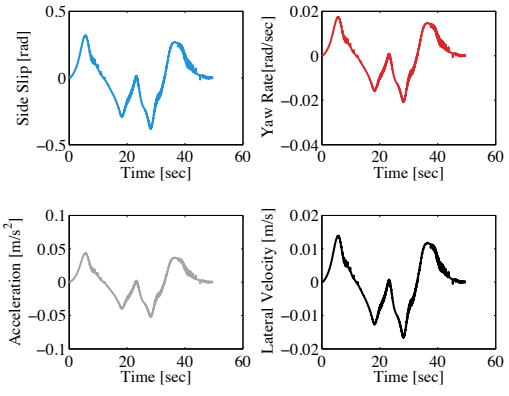

(c) v = 2.5 m/s

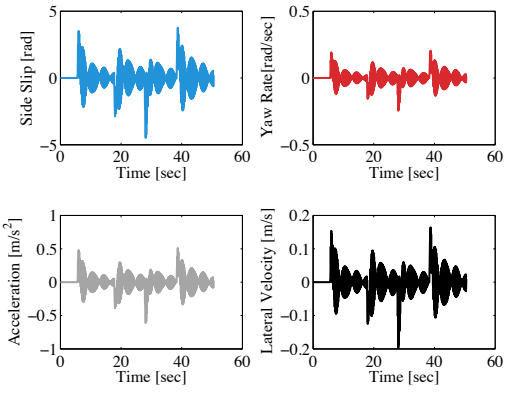

(d) v = 2.5 m/s

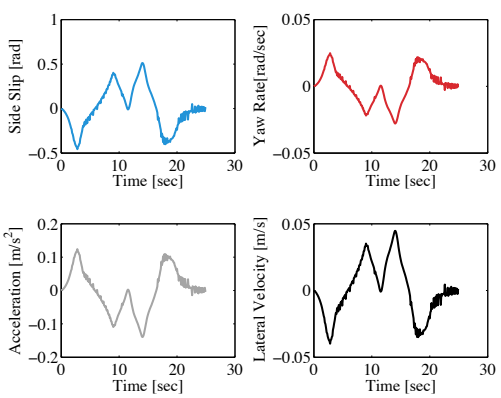

(e) v = 5 m/s

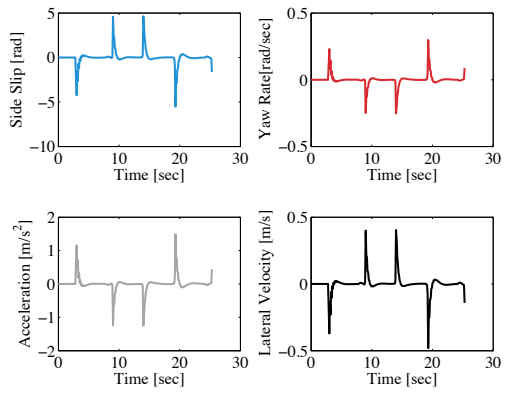

(f) v = 5 m/s

Fig. 9. Case (2) vehicle response to PID tracking control of continuous (a)(c)(e) and discontinuous (b)(d)(f) paths

5. Discussion and Conclusion

The current research presents an empirical performance analysis of the effect of varying path continuity on pure pursuit path tracking controllers. Proportional and PID controllers were implemented for paths of varying configurations. Comparative analyses were conducted between cubic parametrically continuous splines and discontinuous arcs-line concatenations. The experiments were replicated for three different velocities. The presented results validated the expected outcomes, i.e. benefits of continuous paths applications. Tracking errors were significantly reduced with continuous splines, see Fig. 4, for all experimental configurations. Controller effort was also reduced, as a result of having continuous reference paths, see Fig. 5. An analysis of the steady state dynamic steering responses revealed improved stability of the vehicle. In all experiments the side slip angle was reduced in an order of 50-95%, as shown in Fig. 6, Fig. 7, Fig. 8 and Fig. 9. This investigation validates the significance of maintaining continuous paths in order to reduce path tracking errors. The contributions of continuous paths for the vehicle dynamic stability and resulting disturbances minimisation, such as centrifugal acceleration are also revealed. Following that, it is obvious that continuous splines are well suited to generate reference paths, and improve performances of stability control systems, that will be used for autonomous passenger vehicles navigation.

Acknowledgments

M. Elbanhawi acknowledges the financial support of the Australian Postgraduate Award (APA) and Research Training Scheme (RTS).

References

1. Lee JD. Fifty Years of Driving Safety Research. *Human Factors: The Journal of the Human Factors and Ergonomics Society*. 2008; 50: 521-8.
2. Campion G, Bastin G and Dandrea-Novel B. Structural properties and classification of kinematic and dynamic models of wheeled mobile robots. *Robotics and Automation, IEEE Transactions on*. 1996; 12: 47-62.
3. d'Andrea-Novel B, Campion G and Bastin G. Control of Nonholonomic Wheeled Mobile Robots by State Feedback Linearization. *The International Journal of Robotics Research*. 1995; 14: 543-59.
4. Jazar RN. *Vehicle Dynamics: Theory and Application*. Springer, 2008.
5. Marzbani H, Ahmad Salahuddin MH, Simic M, Fard M and Jazar RN. Steady-state dynamic steering. *Frontiers in Artificial Intelligence and Applications*. 2014, p. 493-504.
6. ISO 3888-1 (International Organisation for Standardisation). Passenger cars — Test track for a severe lane-change manoeuvre — Part 1: Double Lane Change. 1999.
7. Elbanhawi M, Simic M and Jazar R. Continuous Path Smoothing for Car-Like Robots Using B-Spline Curves. *J Intell Robot Syst*. 2015: 1-34.
8. Xuan-Nam B, Boissonnat J-d, Soueres P and Laumond JP. Shortest path synthesis for Dubins non-holonomic robot. *Robotics and Automation, 1994 Proceedings, 1994 IEEE International Conference on*. 1994, p. 2-7 vol.1.
9. Roth S and Batavia P. Evaluating Path Tracker Performance for Outdoor Mobile Robots. *Automation Technology for Off-Road Equipment*. Chicago, Illinois, USA: American Society of Agricultural and Biological Engineers, 2002, p. 399-7.
10. Thrun S, Montemerlo M, Dahlkamp H, et al. Stanley: The Robot That Won the DARPA Grand Challenge. In: Buehler M, Iagnemma K and Singh S, (eds.). *The 2005 DARPA Grand Challenge*. Springer Berlin Heidelberg, 2007, p. 1-43.